Review Article

Advanced magnetic resonance imaging in glioblastoma: a review

Gaurav Shukla[1,2], Gregory S. Alexander[1], Spyridon Bakas[2,3], Rahul Nikam[4], Kiran Talekar[4], Joshua D. Palmer[5], Wenyin Shi[1]

[1]Department of Radiation Oncology, Sidney Kimmel Cancer Center, Thomas Jefferson University, Philadelphia, PA, USA; [2]Center for Biomedical Image Computing and Analytics, Perelman School of Medicine, University of Pennsylvania, Richards Medical Research Laboratories, Philadelphia, PA 19104, USA; [3]Department of Radiology, Perelman School of Medicine, University of Pennsylvania, Philadelphia, PA 19104, USA; [4]Department of Radiology, Thomas Jefferson University, Philadelphia, PA, USA; [5]Department of Radiation Oncology, The Ohio State University Wexner Medical Center, Columbus, OH 43215, USA

Contributions: (I) Conception and design: G Shukla, W Shi; (II) Administrative support: None; (III) Provision of study materials or patients: GS Alexander, G Shukla, K Talekar, R Nikam; (IV) Collection and assembly of data: G Shukla, R Nikam; (V) Data analysis and interpretation: All authors; (VI) Manuscript writing: All authors; (VII) Final approval of manuscript: All authors.

Correspondence to: Gaurav Shukla, MD, PhD. Department of Radiation Oncology, Thomas Jefferson University, Philadelphia, PA, USA. Email: gaurav.shukla@jefferson.edu.

Abstract: Glioblastoma, the most common and most rapidly progressing primary malignant tumor of the central nervous system, continues to portend a dismal prognosis, despite improvements in diagnostic and therapeutic strategies over the last 20 years. The standard of care radiographic characterization of glioblastoma is magnetic resonance imaging (MRI), which is a widely utilized examination in the diagnosis and post-treatment management of patients with glioblastoma. Basic MRI modalities available from any clinical scanner, including native T1-weighted (T1w) and contrast-enhanced (T1CE), T2-weighted (T2w), and T2-fluid-attenuated inversion recovery (T2-FLAIR) sequences, provide critical clinical information about various processes in the tumor environment. In the last decade, advanced MRI modalities are increasingly utilized to further characterize glioblastomas more comprehensively. These include multi-parametric MRI sequences, such as dynamic susceptibility contrast (DSC), dynamic contrast enhancement (DCE), higher order diffusion techniques such as diffusion tensor imaging (DTI), and MR spectroscopy (MRS). Significant efforts are ongoing to implement these advanced imaging modalities into improved clinical workflows and personalized therapy approaches. Functional MRI (fMRI) and tractography are increasingly being used to identify eloquent cortices and important tracts to minimize postsurgical neuro-deficits. A contemporary review of the application of standard and advanced MRI in clinical neuro-oncologic practice is presented here.

Keywords: Glioblastoma; radiomics; magnetic resonance imaging (MRI); perfusion; diffusion; spectroscopy; radiation oncology

Submitted May 20, 2017. Accepted for publication Jun 07, 2017.
doi: 10.21037/cco.2017.06.28
View this article at: http://dx.doi.org/10.21037/cco.2017.06.28

Initial diagnosis and surgical management

In 2017, it is estimated that 26,070 patients will be diagnosed with a malignant primary brain tumor in the United States, with more than half having the diagnosis of glioblastoma (1). Most patients with glioblastoma undergo computed tomography of the brain (*Figure 1*) upon initial presentation. Once a mass is identified and hemorrhage is excluded, a contrast-enhanced magnetic resonance imaging (MRI) is typically ordered, with standard T2-weighted (T2w), T2-fluid-attenuated inversion recovery (T2-FLAIR) (*Figure 2*), gradient echo (*Figure 3*), T1-weighted (T1w), and T1-weighted contrast-enhanced (T1CE) sequences (*Figure 4*) (2,3). Many institutions will also capture T2w

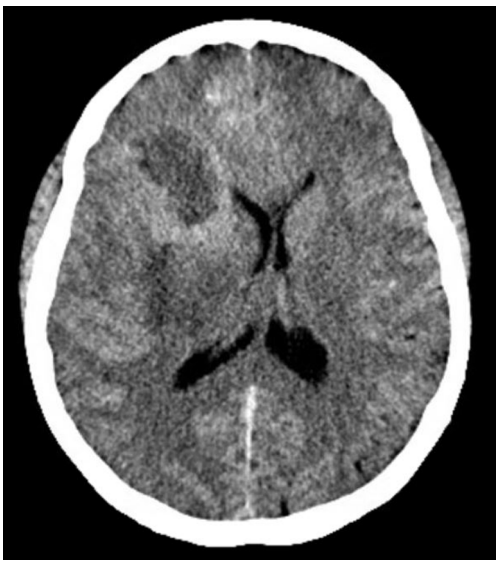

Figure 1 Axial CT image at the level of basal ganglia demonstrates a large heterogeneous mass in the right frontal lobe with mass effect on the right lateral ventricle and leftward shift of midline. CT, computed tomography.

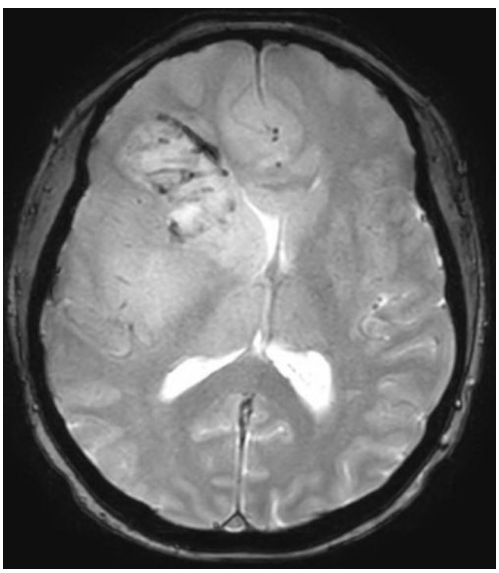

Figure 2 Axial FLAIR weighted image at the level of basal ganglia demonstrates heterogeneous mass centered in the right frontal lobe and basal ganglia with surrounding infiltrating signal abnormality 'FLAIR envelope' which extends medially across the corpus callosum and posteriorly in the insular region. The 'FLAIR envelope' is typically a manifestation of combination of tumor infiltration and edema. There is associated mass effect on the right lateral ventricle and leftward midline shift. FLAIR, fluid-attenuated inversion recovery.

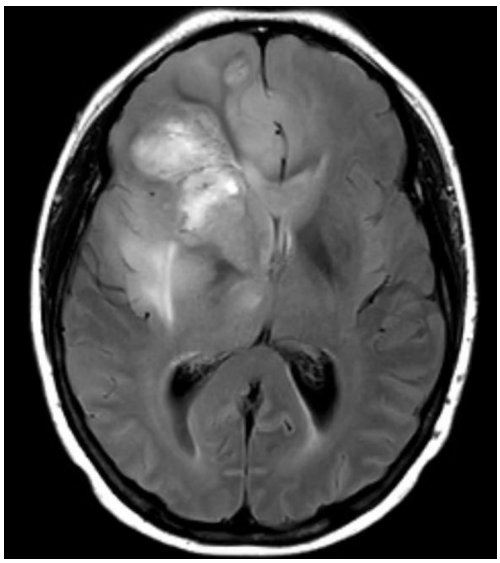

Figure 3 Axial gradient echo (GRE) image depicts multiple foci of hypointense signal 'susceptibility artifacts' within the right frontal mass compatible with intra-tumoral blood products.

gradient echo and diffusion weighted sequences. Maximal safe debulking surgery is typically recommended as the initial standard of care. Neurosurgeons will often utilize high-resolution MRI (0.5–1.2 mm slice thickness) for surgical planning and intraoperative guidance, as well as to make the determination of how aggressively to resect based on risk of toxicity to nearby eloquent regions (4).

Standard imaging also can identify other important characteristics of the mass *in situ*, including the volume of various tumor sub-regions (i.e., necrotic, enhancing, and non-enhancing), compression of the surrounding peritumoral tissue, and midline deviation. The spatial heterogeneity of glioblastoma is macroscopically apparent on standard MRI sequences; beyond the tumor bulk described above, pathology studies demonstrate microscopic tumor infiltration throughout the peritumoral edema, which appears hyperintense on T2-FLAIR sequences (*Figure 2*). More than 90% of tumor recurrences will occur within this T2-FLAIR envelope (5), and there is limited research focused in the assessment of this region and its microenvironment (6). Edema appears to develop in response to angiogenic and vascular permeability factors associated with infiltrating tumor (7,8). As tumors outgrow the native blood supply, the resultant ischemia triggers further secretion of angiogenic factors that promote vascular proliferation (9,10).

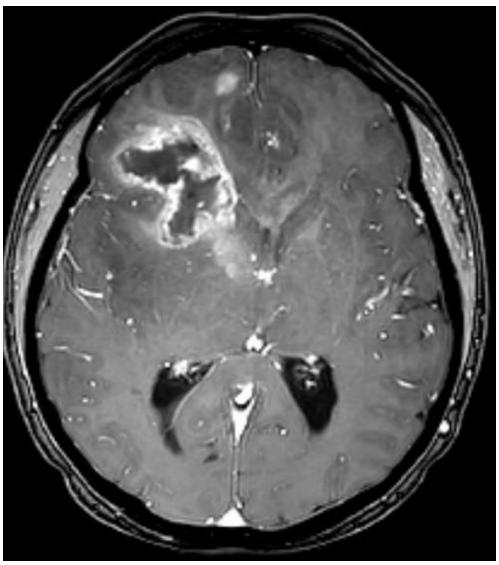

Figure 4 Post gadolinium based contrast administration T1 weighted axial image (T1CE). There is heterogeneous irregular peripheral enhancement associated with the right frontal lobe mass with central non-enhancing area, consistent with necrosis. Of note are additional patchy areas of enhancement in the right anterior frontal lobe and right basal ganglia region. These additional areas of enhancement lie within the previously described region of 'FLAIR envelope'. FLAIR, fluid-attenuated inversion recovery. T1CE, T1-weighted contrast-enhanced.

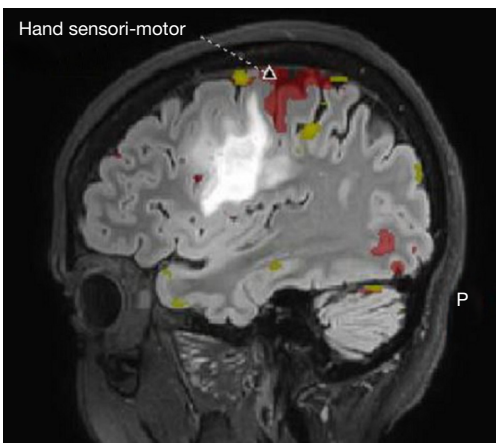

Figure 5 BOLD fMRI for localization of hand sensorimotor cortex in a patient with right frontal glial neoplasm. BOLD fMRI data is superimposed on sagittal FLAIR weighted image for anatomic localization. In the right hemisphere, the hand sensorimotor cortex (arrow) is located along the posterosuperior aspect of the frontal mass and is separated by less than one gyrus distance. fMRI, functional magnetic resonance imaging; FLAIR, fluid-attenuated inversion recovery.

A recent meta-analysis of over 40,000 glioblastoma patients demonstrated that gross-total resection was associated with improved survival as compared to subtotal resection (11). Historically, the determination of gross-total resection was made in the operating room by the neurosurgeon. However, in the modern era, the practice of obtaining a post-operative T1CE MRI within 24–48 hours of surgery has become routine after publication of a study showing that radiological determination of the extent of resection via MRI had prognostic significance (12). Several series have attempted to quantify a threshold value for the extent of resection as a guide for neurosurgeons, utilizing the amount or enhancing tumor present in the preoperative and post-operative T1CE images. These series report thresholds ranging from 70% to 100% (13-15), with the caveats that they were obtained retrospectively. To date, no formal threshold is recommended other than "maximal safe resection" as mentioned previously.

Standard preoperative images can be analyzed for macroscopic shape and location features that are associated with improved survival (16-19), providing potential biomarkers that may be utilized in stratifying patients in clinical trials.

Advanced MRI sequences have utility in the preoperative domain as well. Functional imaging (fMRI) has been particularly useful in preoperative surgical planning in cases where tumors or their resection may disrupt eloquent areas (*Figures 5*-7). Many patients who were once felt to be unresectable due to uncertain risk of neurologic compromise are now candidates for more aggressive resection after functional mapping (20). Diffusion techniques including diffusion tensor imaging (DTI) generates rich white matter tractography images (*Figures 8*,*9*) which may guide neurosurgical planning (21) and can help distinguish between post-operative vascular damage and residual enhancing tumor (22). Dynamic contrast enhancement (DCE) sequences in the preoperative setting measure pharmacokinetic parameters of contrast uptake, which may be associated with early disease progression and survival (23). Dynamic susceptibility contrast (DSC) MRI (*Figure 10*) may be helpful in preoperative diagnosis (24) of malignant lesions. Imaging features (i.e., radiomic features) (25) extracted from standard and advanced preoperative MR sequences via advanced computational methods have shown evidence to predict survival, molecular subtype, and mutational status in glioblastoma (26,27), potentially enhancing the set of imaging biomarkers available to clinicians.

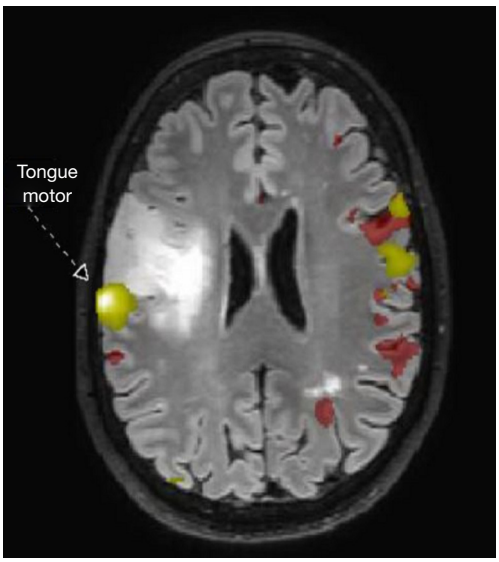

Figure 6 BOLD fMRI for localization of tongue sensorimotor cortex. BOLD fMRI data is superimposed on axial FLAIR weighted image for anatomic localization. In the right hemisphere, the area of activation (arrow), tongue sensorimotor cortex is in immediate proximity of the posterior margin of the right frontal mass. FLAIR envelope seems to extend into this region of activation. fMRI, functional magnetic resonance imaging; FLAIR, fluid-attenuated inversion recovery.

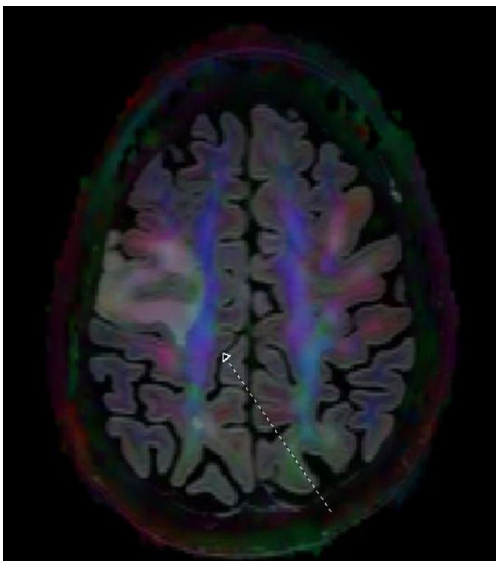

Figure 8 Color fractional anisotropy map superimposed on axial FLAIR weighted image. There is loss of fractional anisotropy in the expected region of right corticospinal tract (arrow, blue colored fibers). This tract is located at the posteromedial margin of the FLAIR envelope. Loss of fractional anisotropy may be related to edema, infiltration by tumor or displacement. FLAIR, fluid-attenuated inversion recovery.

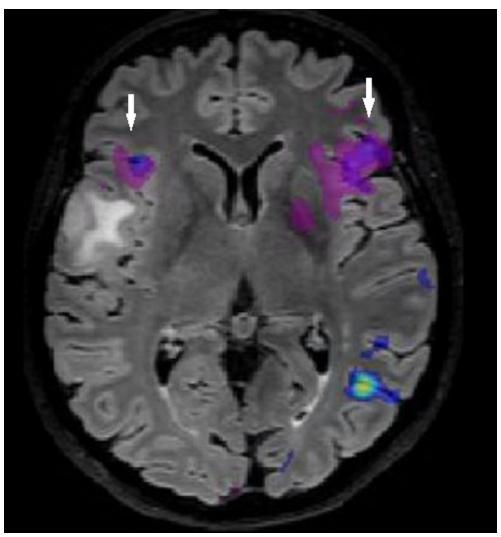

Figure 7 BOLD fMRI for localization of Broca's area in a patient with right frontal glial neoplasm. There is bilateral Broca's area activation on sentence completion and verb generation tasks (arrows), with the right hemispheric area of activation located at the anteroinferior aspect of tumor within one gyrus distance. fMRI, functional magnetic resonance imaging.

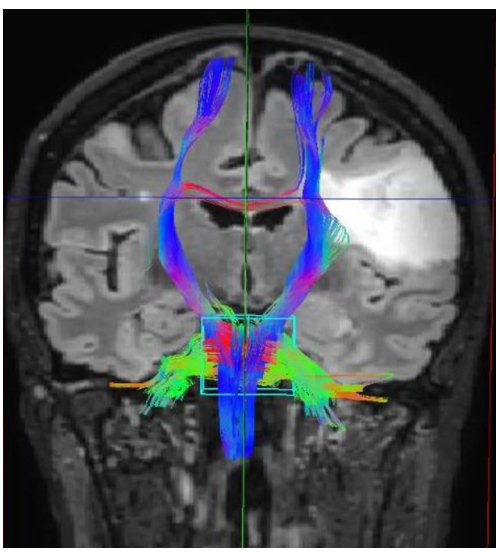

Figure 9 Tractography image demonstrates the intimate relationship of right frontal mass with the corticospinal tract (blue colored fibers).

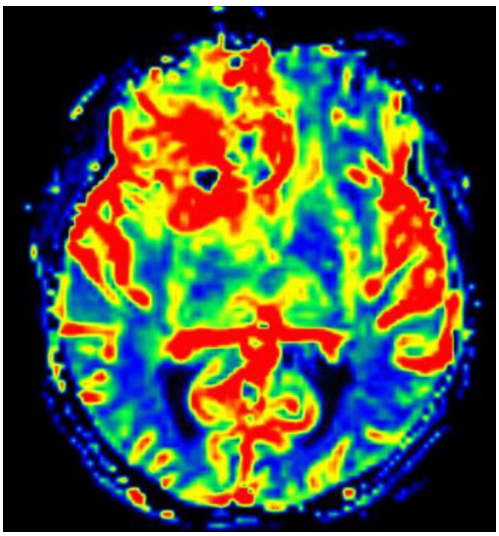

Figure 10 Dynamic susceptibility contrast (DSC) perfusion weighted image. There is increase in rCBV (relative cerebral blood volume) in the region of right frontal mass (*Figures 1-4*), a finding favoring high grade neoplasm.

Post-operative imaging and radiation planning

After maximal safe resection, which is evaluated on immediate post-operative MRI (*Figure 11*), the standard of care for patients with glioblastoma is chemoradiation with concurrent temozolomide, after the results of a large randomized phase III trial (28). Typically, chemoradiation begins 3–6 weeks after surgery to allow for adequate post-operative recovery. Radiotherapy planning includes registration (also known as "fusion") of the post-operative MRI (T1CE and T2-FLAIR sequences) with the planning simulation CT, which allows for delineation of the T2-FLAIR abnormality and residual enhancement in treatment planning. Guidelines for these delineations exist, but substantial variation is observed among practitioners from different cooperative groups [e.g., RTOG (29) *vs.* EORTC (30)], and even among practitioners from one country (31), but all utilize post-operative MRI to define the at-risk target volumes and organs at risk.

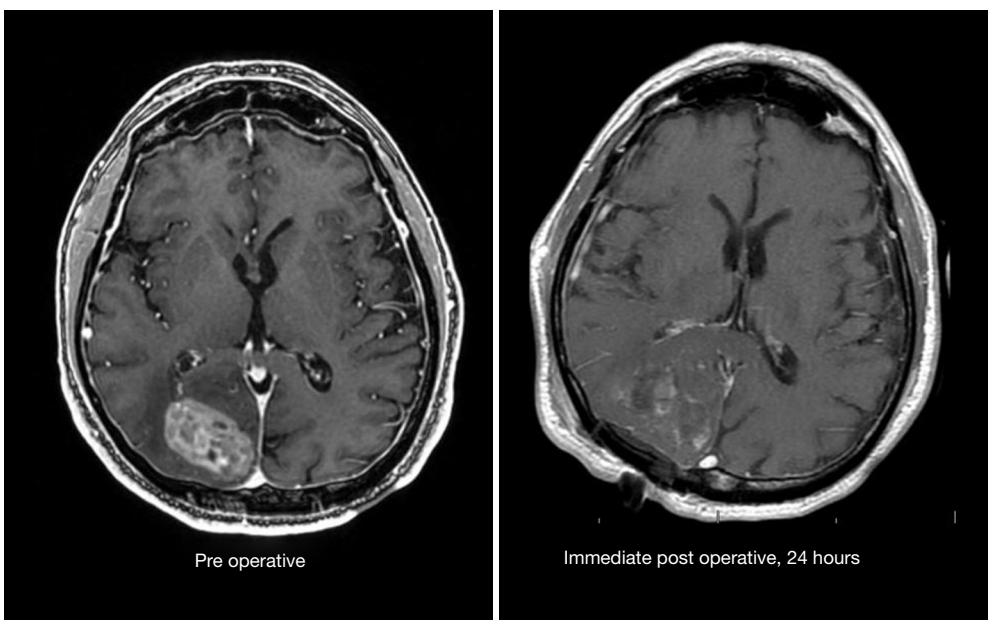

Figure 11 Pre- and immediate post-operative (at 24 hours) axial T1CE weighted images. On post-operative image, there is minimal residual enhancement particularly along the medial aspects of the surgical site, concerning for minimal residual tumor. Majority of the hyperintense signal in the right parieto-occipital region is related to post-operative blood products. T1CE, T1-weighted contrast-enhanced.

The visual assessment of different tumor sub-regions in MRI scans can be very challenging due to anatomic complexity, especially in the post-operative setting. Delineation of targets and critical structures by clinicians is time-consuming and subject to observer bias (32), with reported intra- and inter-rater variability for the determination of glioma boundaries up to 20% and 28%, respectively (33). This variability highlights the rising need for automated brain tumor segmentation that could lead to accurate quantitative assessment of these histologically heterogeneous various tumor sub-regions (34-37), which may benefit clinical workflow in radiology and radiation oncology settings as well as provide platforms for radiomic research.

It is common to identify shifting of brain parenchyma on planning CT in the weeks after craniotomy as the normal brain tissue expands to fill the space taken out by the tumor. One study demonstrated a 4mm shift in the position of the treatment isocenter between CT and MRI-based target delineation (38), even with only a few days between studies. The magnitude of the shift can be several centimeters, resulting in inaccurate registration between post-operative MRI and simulation CT. Many institutions have begun the practice of obtaining repeat MRI at the time of simulation to better characterize the soft tissues for target delineation.

Advanced imaging at this timepoint may play a role in radiation planning. A Polish study demonstrated the discordance between gross tumor volumes (GTVs) delineated from MRI as compared to 18F-fluoroethylthyrosine-positron emission tomography (FET-PET), another functional imaging modality; FET-PET was better associated with the site of eventual failure, suggesting that traditional target volumes may not be adequate (39). Apparent diffusion coefficient (ADC) maps represent measurements generated from diffusion imaging and can identify areas of restricted diffusion that may predict areas of eventual recurrence with high concordance (40,41); along with fractional anisotropy measurements from diffusion images, ADC values may be associated with poor response to treatment and worse survival among high grade glioma patients (42). Diffusion and perfusion parameters, when combined with standard MRI sequences, may allow radiation oncologists to better characterize the highest-risk regions to include in high-dose target volumes, utilizing macroscopically visible features (43) as well as radiomic features (44). Voxel-based MR spectroscopy (MRS) and whole-brain spectroscopic MRI (sMRI) may identify regions of tumor infiltration and areas at high risk of recurrence (*Figure 12*) (45); regions with metabolic abnormalities on sMRI are correlated with intraoperative tissue samples showing increased immunohistochemical staining for neoplastic cells (46).

Response assessment

As demonstrated at any multidisciplinary tumor board, imaging is of utmost importance in the interpretation of the response to treatment in glioblastoma. The first widely-adopted set of guidelines for standardizing the assessment of treatment response that utilized MRI was the Macdonald criteria (47), which used clinical parameters in conjunction with imaging measurements to classify responses into four broad categories (complete response, partial response, stable disease, and progressive disease) (*Figures 13-15*).

Challenges and limitations of the Macdonald criteria became apparent as imaging modalities revealed more details about gliomas and their response to treatment. The importance of non-contrast-enhancing regions of abnormality has become better understood; for example, changes in the volume of hyperintensity on post-treatment T2-FLAIR imaging, relative to baseline, are correlated with improved survival (48) (*Figures 16*,*17*). Furthermore, some glioblastomas demonstrate imaging changes consistent with progression under the Macdonald criteria, but upon repeat surgical intervention, viable tumor cannot be identified in the resection specimen, suggesting that the adjuvant treatment may actually be having a positive effect that eludes detection on conventional imaging. This finding, termed "pseudoprogression", is most commonly observed in patients whose tumors harbored a methylated MGMT promoter region (49), and makes accurate assessment of response difficult, especially in the setting of clinical trials attempting to answer the question of efficacy of novel treatment regimens (*Figure 18*). Some medications, including anti-angiogenic drugs and immunologic agents, elicit unique radiographic changes which may mask accurate response assessment as well.

These limitations, among others, led to the development of a new set of guidelines developed by the Response Assessment in Neuro-Oncology (RANO) (45) working group (50), which incorporates more information from MRI, including T2-FLAIR sequence changes, into the

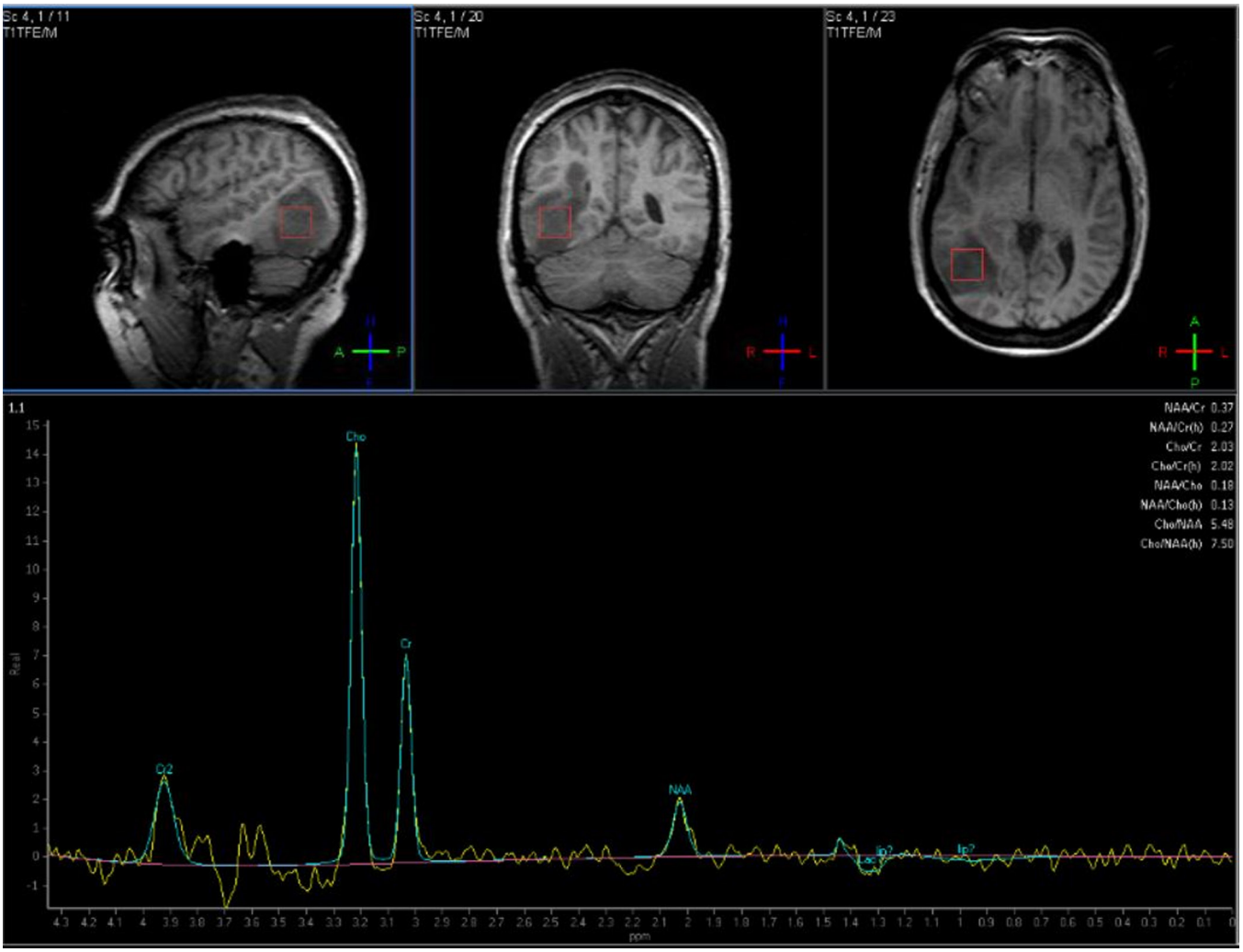

Figure 12 Single voxel MR spectroscopy at long TE (288 ms) acquired through the right temporoparietal region mass with imaging appearance compatible with glial neoplasm. There is markedly elevated choline (resonates at 3.2 ppm) with markedly decreased NAA (resonates at 2 ppm), a finding consistent with high grade glial neoplasm. MR, magnetic resonance.

objective assessment. The RANO criteria have been incorporated into clinical trials and daily clinical practice, allowing more effective comparisons (51).

Clinical trials in the last decade have evaluated bevacizumab, an anti-angiogenic monoclonal antibody, in recurrent glioblastoma (52). The radiographic appearance of malignant gliomas changes dramatically after treatment with bevacizumab as a result of changes in vessel permeability and contrast dynamics (53). Initial studies showed the difficulty in distinguishing these radiographic changes from true tumor effect; the temporal dynamics were also unclear (54).

More recently, immunotherapies have been introduced for treatment of glioblastoma. The radiographic appearance of tumors after immunotherapy demonstrated new challenges with interpretation in the context of prior criteria. This may be due to the uncertainty regarding the temporal dynamics of immunotherapy, as well as the desire for an inflammatory response which may mimic radiologic features of tumor progression. These issues with immunotherapy led to the development of the immunotherapy response assessment in neuro-oncology

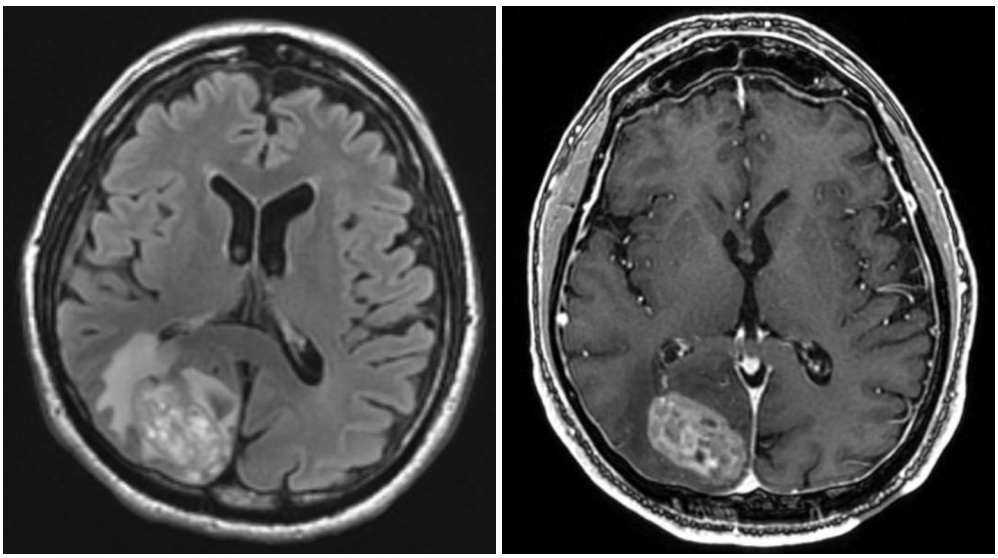

Figure 13 Axial FLAIR and post contrast T1 weighted images demonstrate a large heterogeneously enhancing mass in the right parieto-occipital region with surrounding FLAIR hyperintense signal, compatible with high grade glial neoplasm. FLAIR, fluid-attenuated inversion recovery.

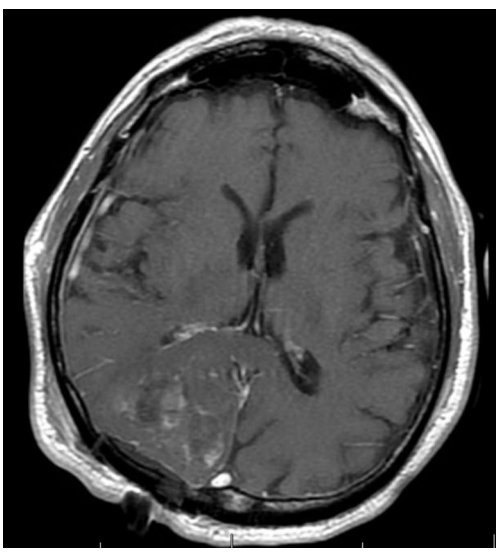

Figure 14 Immediate post-operative (at 24 hours) axial post contrast T1 weighted image. There is minimal residual peripheral enhancement particularly along the medial aspects of the surgical site concerning for small amount of residual tumor.

(iRANO) criteria (55), which attempted to provide standardized guidelines for the determination of tumor progression in the setting of immune-related therapy.

MRI radiomic features have the potential to predict treatment response to specific modalities of treatment (25). Clinically, relative cerebral blood volume and dynamics parameters (K_{trans} and V_e), measured by DSC- and DCE-MRI, may predict treatment response to standard chemoradiation and VEGF inhibitors (56-58), prior to initiation of therapy. Furthermore, radiomic features beyond what can be visually observed in these images have been shown to have predictive value as well (26,27,44,59).

Conclusions

The volume of medical imaging data continues to grow at an exponential rate. As MRI becomes more cost-effective and the adoption of advanced MR modalities becomes more widespread, it will become more critical than ever to incorporate advanced imaging and the power of large datasets into the management of glioblastoma. We anticipate that these changes will include not only the utilization of new MR sequences but also novel image analysis and machine learning techniques, including radiomic analysis, to better drive treatment decision-making in a personalized fashion, with the goal of improving clinical outcomes in glioblastoma.

Acknowledgements

None.

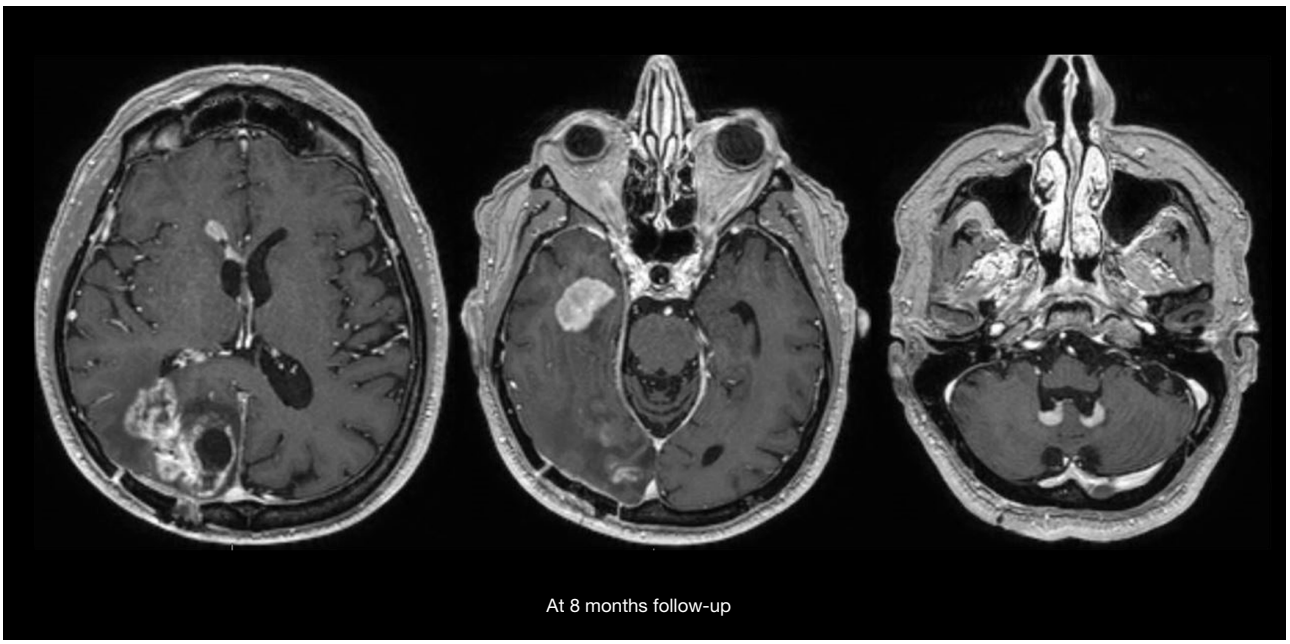

Figure 15 Axial post-contrast T1 (T1CE) images at 8 months. There is a large heterogeneously enhancing mass in the right parieto-occipital region at the operative site. There is interval development of multiple enhancing nodules along the ependymal surface of ventricles, particularly along the right frontal and temporal horn, and roof of fourth ventricles. These findings are compatible with tumor progression. T1CE, T1-weighted contrast-enhanced.

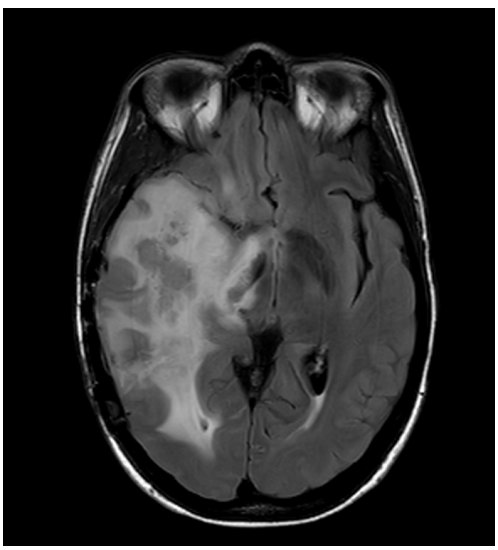

Figure 16 Follow up of a case of glioblastoma on therapy. Axial FLAIR weighted image demonstrates a large area of infiltrating hyperintense signal abnormality in right temporo-occipital region, with associated mass effect and leftwards shift of midline. FLAIR, fluid-attenuated inversion recovery.

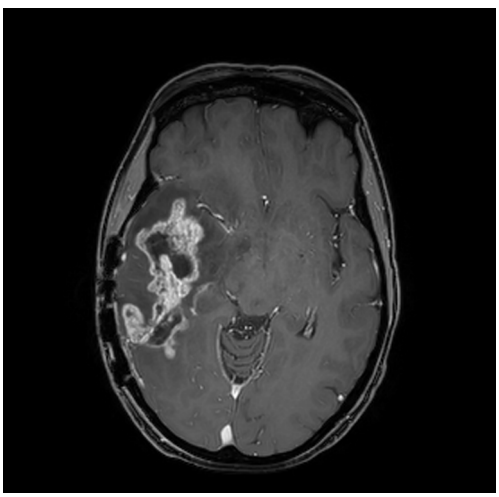

Figure 17 Axial T1CE image depicts an area of heterogeneous enhancement in right temporal lobe within the region of FLAIR signal abnormality. FLAIR, fluid-attenuated inversion recovery. T1CE, T1-weighted contrast-enhanced.

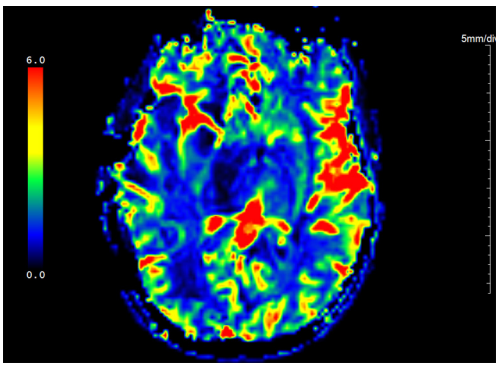

Figure 18 On dynamic susceptibility contrast (DSC) perfusion weighted imaging, the area of signal abnormality predominantly demonstrates low relative cerebral blood volumes. The overall findings were consistent with pseudoprogression.

Footnote

Conflicts of Interest: The authors have no conflicts of interest to declare.

References

1. Ostrom QT, Gittleman H, de Blank PM, et al. American Brain Tumor Association Adolescent and Young Adult Primary Brain and Central Nervous System Tumors Diagnosed in the United States in 2008-2012. Neuro Oncol 2016;18 Suppl 1:i1-i50.
2. Cha S. Update on brain tumor imaging: from anatomy to physiology. AJNR Am J Neuroradiol 2006;27:475-87.
3. Young GS. Advanced MRI of adult brain tumors. Neurol Clin 2007;25:947-73, viii.
4. Price SJ, Gillard JH. Imaging biomarkers of brain tumour margin and tumour invasion. Br J Radiol 2011;84 Spec No 2:S159-67.
5. Petrecca K, Guiot MC, Panet-Raymond V, et al. Failure pattern following complete resection plus radiotherapy and temozolomide is at the resection margin in patients with glioblastoma. J Neurooncol 2013;111:19-23.
6. Lemee JM, Clavreul A, Menei P. Intratumoral heterogeneity in glioblastoma: don't forget the peritumoral brain zone. Neuro Oncol 2015;17:1322-32.
7. Chang EL, Akyurek S, Avalos T, et al. Evaluation of peritumoral edema in the delineation of radiotherapy clinical target volumes for glioblastoma. Int J Radiat Oncol Biol Phys 2007;68:144-50.
8. Akbari H, Macyszyn L, Da X, et al. Pattern analysis of dynamic susceptibility contrast-enhanced MR imaging demonstrates peritumoral tissue heterogeneity. Radiology 2014;273:502-10.
9. Bullitt E, Zeng D, Gerig G, et al. Vessel tortuosity and brain tumor malignancy: a blinded study. Acad Radiol 2005;12:1232-40.
10. Kerbel RS. Tumor angiogenesis: past, present and the near future. Carcinogenesis 2000;21:505-15.
11. Brown TJ, Brennan MC, Li M, et al. Association of the Extent of Resection With Survival in Glioblastoma: A Systematic Review and Meta-analysis. JAMA Oncol 2016;2:1460-9.
12. Albert FK, Forsting M, Sartor K, et al. Early postoperative magnetic resonance imaging after resection of malignant glioma: objective evaluation of residual tumor and its influence on regrowth and prognosis. Neurosurgery 1994;34:45-60; discussion -1.
13. Lacroix M, Abi-Said D, Fourney DR, et al. A multivariate analysis of 416 patients with glioblastoma multiforme: prognosis, extent of resection, and survival. J Neurosurg 2001;95:190-8.
14. Stummer W, Reulen HJ, Meinel T, et al. Extent of resection and survival in glioblastoma multiforme: identification of and adjustment for bias. Neurosurgery 2008;62:564-76; discussion -76.
15. Sanai N, Berger MS. Operative techniques for gliomas and the value of extent of resection. Neurotherapeutics 2009;6:478-86.
16. Wangaryattawanich P, Hatami M, Wang J, et al. Multicenter imaging outcomes study of The Cancer Genome Atlas glioblastoma patient cohort: imaging predictors of overall and progression-free survival. Neuro Oncol 2015;17:1525-37.
17. Archive TCI. VASARI Research Project. Available online: https://wiki.cancerimagingarchive.net/display/Public/VASARI+Research+Project. Accessed 5/3/2017.
18. Perez-Beteta J, Martinez-Gonzalez A, Molina D, et al. Glioblastoma: does the pre-treatment geometry matter? A postcontrast T1 MRI-based study. Eur Radiol 2017;27:1096-104.
19. Czarnek N, Clark K, Peters KB, et al. Algorithmic three-dimensional analysis of tumor shape in MRI improves prognosis of survival in glioblastoma: a multi-institutional study. J Neurooncol 2017;132:55-62.
20. Sanai N, Mirzadeh Z, Berger MS. Functional outcome after language mapping for glioma resection. N Engl J Med 2008;358:18-27.
21. Abdullah KG, Lubelski D, Nucifora PG, et al. Use of diffusion tensor imaging in glioma resection. Neurosurg

Focus 2013;34:E1.
22. Lee SK. Diffusion tensor and perfusion imaging of brain tumors in high-field MR imaging. Neuroimaging Clin N Am 2012;22:123-34, ix.
23. Kim R, Choi SH, Yun TJ, et al. Prognosis prediction of non-enhancing T2 high signal intensity lesions in glioblastoma patients after standard treatment: application of dynamic contrast-enhanced MR imaging. Eur Radiol 2017;27:1176-85.
24. Chakravorty A, Steel T, Chaganti J. Accuracy of percentage of signal intensity recovery and relative cerebral blood volume derived from dynamic susceptibility-weighted, contrast-enhanced MRI in the preoperative diagnosis of cerebral tumours. Neuroradiol J 2015;28:574-83.
25. Aerts HJ. The Potential of Radiomic-Based Phenotyping in Precision Medicine: A Review. JAMA Oncol 2016;2:1636-42.
26. Bakas S, Akbari H, Pisapia J, et al. In vivo detection of EGFRvIII in glioblastoma via perfusion magnetic resonance imaging signature consistent with deep peritumoral infiltration: the φ index. Clin Cancer Res 2017. [Epub ahead of print].
27. Macyszyn L, Akbari H, Pisapia JM, et al. Imaging patterns predict patient survival and molecular subtype in glioblastoma via machine learning techniques. Neuro Oncol 2016;18:417-25.
28. Stupp R, Hegi ME, Mason WP, et al. Effects of radiotherapy with concomitant and adjuvant temozolomide versus radiotherapy alone on survival in glioblastoma in a randomised phase III study: 5-year analysis of the EORTC-NCIC trial. Lancet Oncol 2009;10:459-66.
29. Gilbert MR, Wang M, Aldape KD, et al. Dose-dense temozolomide for newly diagnosed glioblastoma: a randomized phase III clinical trial. J Clin Oncol 2013;31:4085-91.
30. Stupp R, Mason WP, van den Bent MJ, et al. Radiotherapy plus concomitant and adjuvant temozolomide for glioblastoma. N Engl J Med 2005;352:987-96.
31. Wee CW, Sung W, Kang HC, et al. Evaluation of variability in target volume delineation for newly diagnosed glioblastoma: a multi-institutional study from the Korean Radiation Oncology Group. Radiat Oncol 2015;10:137.
32. Deeley MA, Chen A, Datteri R, et al. Comparison of manual and automatic segmentation methods for brain structures in the presence of space-occupying lesions: a multi-expert study. Phys Med Biol 2011;56:4557-77.
33. Mazzara GP, Velthuizen RP, Pearlman JL, et al. Brain tumor target volume determination for radiation treatment planning through automated MRI segmentation. Int J Radiat Oncol Biol Phys 2004;59:300-12.
34. Bakas S, Zeng K, Sotiras A, et al. GLISTRboost: Combining Multimodal MRI Segmentation, Registration, and Biophysical Tumor Growth Modeling with Gradient Boosting Machines for Glioma Segmentation. In: Crimi A, Menze B, Maier O, et al. editors. Brainlesion: Glioma, Multiple Sclerosis, Stroke and Traumatic Brain Injuries. Lecture Notes in Computer Science 2016;9556:144-55.
35. Zeng K, Bakas S, Sotiras A, et al. Segmentation of Gliomas in Pre-operative and Post-operative Multimodal Magnetic Resonance Imaging Volumes Based on a Hybrid Generative-Discriminative Framework. In: Crimi A, Menze B, Maier O, et al. editors. Brainlesion: Glioma, Multiple Sclerosis, Stroke and Traumatic Brain Injuries. Lecture Notes in Computer Science 2017;10154.
36. Menze BH, Jakab A, Bauer S, et al. The Multimodal Brain Tumor Image Segmentation Benchmark (BRATS). IEEE Trans Med Imaging 2015;34:1993-2024.
37. Bakas S, Zeng K, Sotiras A, et al. Segmentation of Gliomas in Multimodal Magnetic Resonance Imaging Volumes Based on a Hybrid Generative-Discriminative Framework. In: Menze B, Reyes M, Farahani K, et al. editors. Proceedings of the Multimodal Brain Tumor Image Segmentation Challenge held in conjunction with MICCAI 2015 (MICCAI-BRATS 2015). Munich, Germany: Technische Universität München (T.U.M.), 2015:5-12.
38. Bagri PK, Kapoor A, Singh D, et al. Addition of magnetic resonance imaging to computed tomography-based three-dimensional conformal radiotherapy planning for postoperative treatment of astrocytomas: Changes in tumor volume and isocenter shift. South Asian J Cancer 2015;4:18-20.
39. Harat M, Malkowski B, Makarewicz R. Pre-irradiation tumour volumes defined by MRI and dual time-point FET-PET for the prediction of glioblastoma multiforme recurrence: A prospective study. Radiother Oncol 2016;120:241-7.
40. Elson A, Paulson E, Bovi J, et al. Evaluation of pre-radiotherapy apparent diffusion coefficient (ADC): patterns of recurrence and survival outcomes analysis in patients treated for glioblastoma multiforme. J Neurooncol 2015;123:179-88.
41. Jeong D, Malalis C, Arrington JA, et al. Mean apparent diffusion coefficient values in defining radiotherapy planning target volumes in glioblastoma. Quant Imaging

Med Surg 2015;5:835-45.
42. Qu J, Qin L, Cheng S, et al. Residual low ADC and high FA at the resection margin correlate with poor chemoradiation response and overall survival in high-grade glioma patients. Eur J Radiol 2016;85:657-64.
43. Guo L, Wang G, Feng Y, et al. Diffusion and perfusion weighted magnetic resonance imaging for tumor volume definition in radiotherapy of brain tumors. Radiat Oncol 2016;11:123.
44. Akbari H, Macyszyn L, Da X, et al. Imaging Surrogates of Infiltration Obtained Via Multiparametric Imaging Pattern Analysis Predict Subsequent Location of Recurrence of Glioblastoma. Neurosurgery 2016;78:572-80.
45. Deviers A, Ken S, Filleron T, et al. Evaluation of the lactate-to-N-acetyl-aspartate ratio defined with magnetic resonance spectroscopic imaging before radiation therapy as a new predictive marker of the site of relapse in patients with glioblastoma multiforme. Int J Radiat Oncol Biol Phys 2014;90:385-93.
46. Cordova JS, Shu HK, Liang Z, et al. Whole-brain spectroscopic MRI biomarkers identify infiltrating margins in glioblastoma patients. Neuro Oncol 2016;18:1180-9.
47. Macdonald DR, Cascino TL, Schold SC Jr, et al. Response criteria for phase II studies of supratentorial malignant glioma. J Clin Oncol 1990;8:1277-80.
48. Grossman R, Shimony N, Shir D, et al. Dynamics of FLAIR Volume Changes in Glioblastoma and Prediction of Survival. Ann Surg Oncol 2017;24:794-800.
49. Brandes AA, Franceschi E, Tosoni A, et al. MGMT promoter methylation status can predict the incidence and outcome of pseudoprogression after concomitant radiochemotherapy in newly diagnosed glioblastoma patients. J Clin Oncol 2008;26:2192-7.
50. Wen PY, Macdonald DR, Reardon DA, et al. Updated response assessment criteria for high-grade gliomas: response assessment in neuro-oncology working group. J Clin Oncol 2010;28:1963-72.
51. Chinot OL, Macdonald DR, Abrey LE, et al. Response assessment criteria for glioblastoma: practical adaptation and implementation in clinical trials of antiangiogenic therapy. Curr Neurol Neurosci Rep 2013;13:347.
52. Kreisl TN, Kim L, Moore K, et al. Phase II trial of single-agent bevacizumab followed by bevacizumab plus irinotecan at tumor progression in recurrent glioblastoma. J Clin Oncol 2009;27:740-5.
53. Pope WB, Lai A, Nghiemphu P, et al. MRI in patients with high-grade gliomas treated with bevacizumab and chemotherapy. Neurology 2006;66:1258-60.
54. Ananthnarayan S, Bahng J, Roring J, et al. Time course of imaging changes of GBM during extended bevacizumab treatment. J Neurooncol 2008;88:339-47.
55. Okada H, Weller M, Huang R, et al. Immunotherapy response assessment in neuro-oncology: a report of the RANO working group. Lancet Oncol 2015;16:e534-42.
56. Bennett IE, Field KM, Hovens CM, et al. Early perfusion MRI predicts survival outcome in patients with recurrent glioblastoma treated with bevacizumab and carboplatin. J Neurooncol 2017;131:321-9.
57. O'Neill AF, Qin L, Wen PY, et al. Demonstration of DCE-MRI as an early pharmacodynamic biomarker of response to VEGF Trap in glioblastoma. J Neurooncol 2016;130:495-503.
58. Khalifa J, Tensaouti F, Chaltiel L, et al. Identification of a candidate biomarker from perfusion MRI to anticipate glioblastoma progression after chemoradiation. Eur Radiol 2016;26:4194-203.
59. Kickingereder P, Gotz M, Muschelli J, et al. Large-scale Radiomic Profiling of Recurrent Glioblastoma Identifies an Imaging Predictor for Stratifying Anti-Angiogenic Treatment Response. Clin Cancer Res 2016;22:5765-71.

Cite this article as: Shukla G, Alexander GS, Bakas S, Nikam R, Talekar K, Palmer JD, Shi W. Advanced magnetic resonance imaging in glioblastoma: a review. Chin Clin Oncol 2017;6(4):40. doi: 10.21037/cco.2017.06.28

